

FAR-RED EMISSION OF $\text{CaYAlO}_4:\text{Mn}^{4+}$ SYNTHESIZED BY CO-PRECIPIATION METHOD[#]

L. Q. Duong¹, N. V. Quang², D. H. Nguyen^{1,*}

¹*Advanced Institute for Science and Technology (AIST), Hanoi University of Science and Technology (HUST), 01 Dai Co Viet street, Ha Noi, Viet Nam*

²*Hanoi Pedagogical University 2, Phuc Yen, Ha Noi, Viet Nam*

*Email: hung.nguyenduy@hust.edu.vn

Received: 16 July 2019; Accepted for publication: 6 February 2020

Abstract. Light absorption of the most plants is in range of blue (440 nm), deep-red (660 nm) and far-red around 700-740 nm. The deep-red and far-red light play important roles in reactions of photomorphogenesis of plants. Although red emission phosphors have been researched extensively for white light-emitting diodes, deep-red and far-red emission phosphors for plant growth have been reported inadequately. Thus, in this work, far-red emitting $\text{CaYAlO}_4:\text{Mn}^{4+}$ phosphor was synthesized by co-precipitation method coupled with various annealing temperature from 800 °C to 1300 °C for 5 h. The crystal structure, morphology, and photoluminescence properties of $\text{CaYAlO}_4:\text{Mn}^{4+}$ phosphors were investigated in detail. The crystallinity of the phosphor belongs to tetragonal system with space group I4/mmm. Y^{3+} and Ca^{2+} ions are coordinated by nine oxygen atoms to form $[\text{YO}_9]$ and $[\text{CaO}_9]$ polyhedrons, and the Al^{3+} ions are coordinated by six oxygen atoms forming $[\text{AlO}_6]$ octahedrons that provided suitable sites for Mn^{4+} ions. The obtained sample showed an irregular surface morphology with micro size particles. Under the excitation of 320 nm light, $\text{CaYAlO}_4:\text{Mn}^{4+}$ phosphors gave bright far-red emission around 710 nm due to the ${}^2E_g \rightarrow {}^4A_{2g}$ transition of Mn^{4+} ions. The critical concentration of Mn^{4+} doped in CaYAlO_4 host lattice is 0.5 mol.%. The results show that the $\text{CaYAlO}_4:\text{Mn}^{4+}$ phosphors may be applied to indoor plant growth illumination.

Keywords: $\text{CaYAlO}_4:\text{Mn}^{4+}$, far-red emitting phosphor, plant growth, LED.

Classification numbers: 2.1.1, 2.5.1.

1. INTRODUCTION

Artificial lighting is an important factor for indoor plant growth in agricultural area. Previous studies demonstrated that blue light around 440 nm (400–500 nm), deep-red light around 660 nm (620–690 nm), and far-red light around (700–740 nm) play important roles in reactions of photosynthesis, phototropism and photomorphogenesis, which then have great effects on the growth, development, and edible quality of plants. Recently, light-emitting diodes

[#] Presented at the 11th National Conference on Solid State Physics & Materials Science, Quy Nhon 11-2019.

(LEDs) have attracted significant attention because of their small size and weight, durability, solid-state construction, wavelength specificity, long operational life, and consumption of much less energy [1-4]. LEDs can usually provide specific quality and quantity of light, the control of spectral composition, the adjustments of light intensity, and the high light levels with low radiant heat output in the plant cultivation [5]. Currently, the commercial white LEDs made primarily on the combination of blue InGaN chip, yellow YAG:Ce³⁺ and red phosphor. However, most yellow and red light from the commercial white LEDs is not suitable for photosynthesis process of plant. Thus, it is urgent to develop high-efficiency far-red-emitting phosphors with emission around 700-740 nm for indoor plant growth LEDs. Recently, red phosphors for white LEDs based on fluoride host material doped with transitional metal Mn⁴⁺ ions were widely studied for LED-based devices because that their raw materials are lower-cost than rare-earth-doped materials. However, the red emission is out of absorption region for photosynthesis of plant. Thus, it needs to develop phosphor which meets requirement for plant growth. It is well known that Mn⁴⁺ ion in octahedral coordination environment of oxide host lattice may exhibit broad and strong absorption in the range of 200 – 550 nm due to the ⁴A₂ → (⁴T₁, ²T₂, and ⁴T₂) transitions of Mn⁴⁺ ion, and emit deep-red or far-red light owing to the ²E → ⁴A₂ transition of Mn⁴⁺ ion [6,7]. The emission of Mn⁴⁺ ion can be modified by changing host lattice because it is strongly influenced by the covalence of “Mn⁴⁺ ligand” bonding [8]. In fact, aluminates have been selected as the host materials for Mn⁴⁺-doped red phosphors, because of their various crystal structures, low cost, high chemical, physical stability, and high luminescence efficiency, such as Ca₁₄Zn₆Al₁₀O₃₅:Mn⁴⁺, CaGdAlO₄:Mn⁴⁺, and CaMg₂Al₁₆O₂₇:Mn⁴⁺ [9-12].

Therefore, in this work we chose CaYAlO₄ compound as the host material for Mn⁴⁺ ions doping because it has the structure and contained abundant [AlO₆] octahedrons that may provide suitable sites for Mn⁴⁺ ions since the radius of Mn⁴⁺ ions ($r = 0.530 \text{ \AA}$, coordination number (CN) = 6) is close to that of Al³⁺ ions ($r = 0.535 \text{ \AA}$, CN = 6) [13]. Herein, far-red emitting CaYAlO₄:Mn⁴⁺ phosphor was synthesized by co-precipitation method. The crystal structure, morphology, and luminescent properties of the CaYAlO₄:Mn⁴⁺ phosphors were studied in detail by X-ray diffraction (XRD), FESEM, photoluminescence excitation (PLE) and PL spectra.

2. MATERIALS AND METHODS

2.1. Materials and preparation

In this work, far-red emitting CaYAlO₄:Mn⁴⁺ phosphor was successfully synthesized by co-precipitation method. The starting materials were metal nitrates: Ca(NO₃)₂·4H₂O, Al(NO₃)₃·9H₂O, Mn(NO₃)₂, and Y₂O₃ (≥ 99.9 % purity). The solution of NH₃ (99.9 %) was used as the precipitant. First, Y₂O₃, Ca(NO₃)₂·4H₂O, Al(NO₃)₃·9H₂O, Mn(NO₃)₂ were weighed based on the stoichiometric ratio. Y₂O₃ was dissolved in HNO₃ resulting in the formation of a colorless solution of Y(NO₃)₃ and other materials were mixed with solution of Y(NO₃)₃. The mixed salts were dissolved in 50 ml of DI water. Then, an excess of NH₃ solution was added to create a precipitate solution. pH level of the solution was controlled at 10 pH to precipitate completely. The solution of the precipitate was dried at 200 °C for 15 h to remove the water. Finally, the dried powder was calcined at various temperatures from 800 °C to 1300 °C for 5 h.

2.2. Characterization

The crystal structures of the calcined samples were characterized using X-ray diffraction, carried out on the device (XRD, Bruker D8 Advanced) using Cu K α radiation ($\lambda = 1.5406 \text{ \AA}$). The morphology of the material was investigated by a field emission scanning electron

microscopy (FESEM - JEOL JSM-7600F). The photoluminescence (PL) and photoluminescence excitation (PLE) spectra were measured by NanoLog spectroscopy (Horiba Jobin Yvon) equipped with a 450 W Xenon lamp as an excitation source. All the measurements were performed at room temperature.

3. RESULTS AND DISCUSSION

3.1. Phase purity and crystal structure

The XRD patterns of $\text{CaYAlO}_4:0.5\% \text{Mn}^{4+}$ powders calcined at different temperatures from 800 °C to 1300 °C for 5 h are shown in Fig. 1. As can be seen, all the observed diffraction peaks are in good agreement with JCPDS card No. 81-0742. The CaYAlO_4 belongs to tetragonal crystal system with space group $I4/mmm$ and $a = 3.6750(5) \text{ \AA}$, $c = 12.011(2) \text{ \AA}$, $c/a = 3.2683$, $V = 162.22(4) \text{ \AA}^3$, $Z = 2$ [14]. Y^{3+} and Ca^{2+} ions were coordinated by nine oxygen atoms to form $[\text{YO}_9]$ and $[\text{CaO}_9]$ polyhedrons, and the Al^{3+} ions were coordinated by six oxygen atoms forming $[\text{AlO}_6]$ octahedrons. It is reported that the effective ionic radius of Ca^{2+} ion ($CN = 9$), Y^{3+} ion ($CN = 9$), Al^{3+} ion ($CN = 6$) and Mn^{4+} ion ($CN = 6$) are 1.18 Å, 1.075 Å, 0.535 Å and 0.530 Å, respectively [15]. It is obvious that the ionic radius of Mn^{4+} is close to Al^{3+} and smaller than Ca^{2+} or Y^{3+} , suggesting that Mn^{4+} ions prefer to occupy Al^{3+} site in the host lattice CaYAlO_4 . Besides the diffraction peaks which correspond to the CaYAlO_4 phase, several other peaks at $2\theta = 29.14^\circ$, 31.48° and 48.5° in the XRD patterns are indexed according to the standard JCPDS card no. 041-1105 of Y_2O_3 phase. However, the analytical results show that when the temperature increases, the width and intensity of the diffraction peaks of the CaYAlO_4 phase were reduced and increased, respectively. These results have been confirmed that the annealing temperature increases, the crystallinity of the phosphor enhances, particle size may become larger.

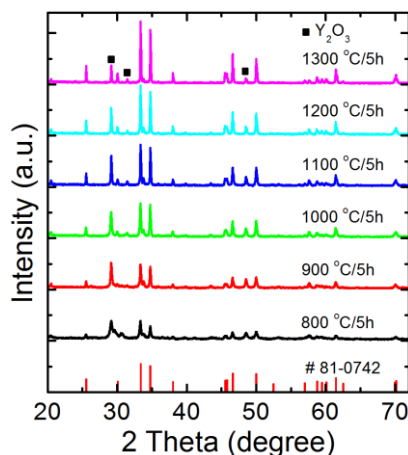


Figure 1. XRD patterns of $\text{CaYAlO}_4:0.5\% \text{Mn}$ powders calcined at different temperatures for 5 h.

3.2. Morphology

Figure 2 shows the FESEM images of $\text{CaYAlO}_4:0.5\% \text{Mn}$ powders calcined at different temperatures 800 °C, 1100 °C, 1200 °C, and 1300 °C. As observed from the images, it is easily observed the size increasing gradually with annealing temperature. The particle size is about

hundreds of nm with annealing temperature to 1200 °C. Their size increase to 1 μm when the sample was annealed at 1300 °C.

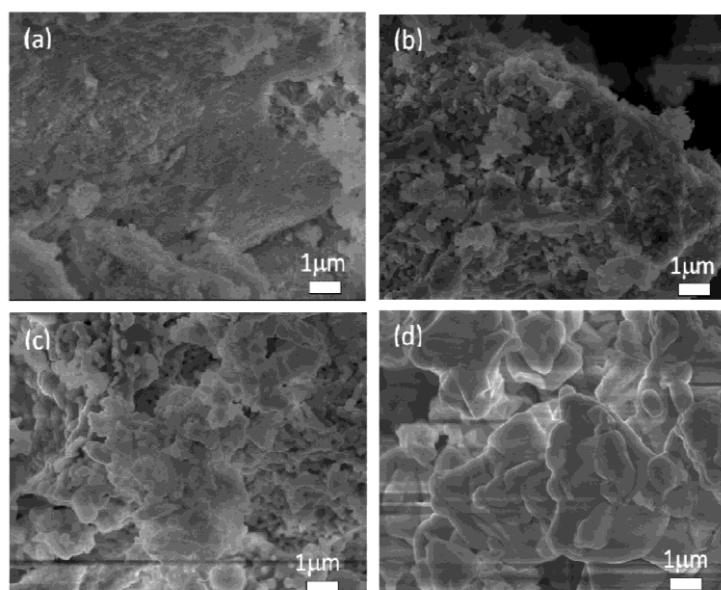


Figure 2. FESEM images of CaYAlO₄:0.5% Mn powders calcined at different temperatures: (a) 800 °C, (b) 1100 °C, (c) 1200 °C and (d) 1300 °C.

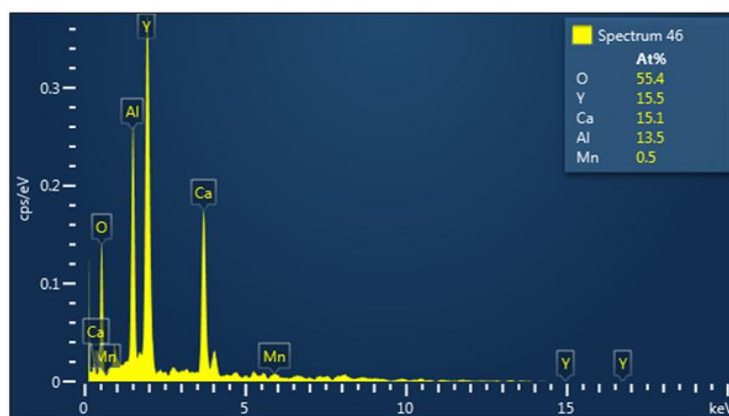


Figure 3. EDX spectrum of CaYAlO₄:0.5%Mn annealed at 1300 °C for 5 h.

Figure 3 shows the EDX spectrum of CaYAlO₄:0.5%Mn⁴⁺ annealed at 1300 °C for 5 h. The spectrum shows the peaks of O, Y, Ca, Al, and Mn with atomic percentage of O : 55.4, Y : 15.5, Ca : 15.1, Al : 13.5, and Mn : 0.5. From the atomic ratio of the sample, it can be confirmed that the content is approximate to those of the prepared CaYAlO₄:0.5%Mn⁴⁺ phosphor. The ratio also demonstrates that the as-prepared phosphor is pure phase as the analysis result of XRD pattern.

3.3. Photoluminescence properties

Figure 4 presents the PLE and PL spectra of $\text{CaYAlO}_4:\text{Mn}^{4+}$ sample. The PLE spectrum was obtained by monitoring at center of emission peak of 710 nm. The PLE spectrum which was measured from 250 to 600 nm includes two broad bands peaking at 320 and 480 nm, which are due to the Mn^{4+} spin-allowed transitions of ${}^4A_{2g} \rightarrow {}^4T_{1g}$, and ${}^4A_{2g} \rightarrow {}^4T_{2g}$, respectively [16]. The PL spectra under the excitation at 320 nm, the $\text{CaYAlO}_4:\text{Mn}^{4+}$ phosphors exhibited strong far-red emissions in the wavelength range of 600–850 nm peaked at 710 nm, which is attributed to the spin forbidden ${}^2E_g \rightarrow {}^4A_{2g}$ transition of Mn^{4+} ions [16]. It is obvious that the phosphor can be effectively excited by UV or blue LED chip and emits red light.

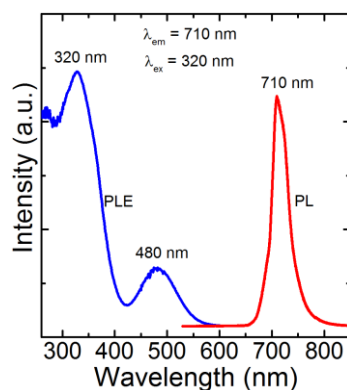


Figure 4. PLE and PL spectra of $\text{CaYAlO}_4:\text{Mn}^{4+}$ phosphors.

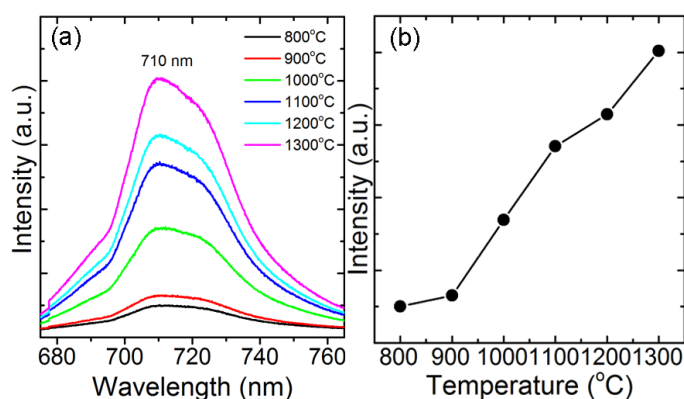


Figure 5. (a) PL spectra of $\text{CaYAlO}_4:0.5\%\text{Mn}$ phosphors calcined at different temperatures: 800 °C – 1300 °C and excited at 320 nm, (b) PL intensity at 710 nm as function of annealing temperature.

Figure 5 shows the emission spectra and PL intensity as a function of annealing temperature of $\text{CaYAlO}_4:\text{Mn}^{4+}$ phosphors under 320 nm excitation. It observes that the PL intensity of the samples at 710 nm enhances with increasing annealing temperature. This result is due to the improvement of crystallinity of particles and homogeneous distribution of Mn^{4+} ions in CaYAlO_4 lattice, which was indicated in the XRD patterns.

To further optimize the red emission of $\text{CaYAlO}_4:\text{Mn}^{4+}$, the phosphor was doped with various concentration of Mn^{4+} . Fig. 6 shows PL spectra and intensity of the $\text{CaYAl}_{1-x}\text{O}_4:x\text{Mn}^{4+}$ ($x = 0.1, 0.3, 0.5, 0.7, 1, \text{ and } 1.5 \text{ mol.}\%$). It is clearly found that the emission intensity at emission peak

710 nm of the phosphors reach a maximum at $x = 0.5$ mol.% and decrease when the concentration of Mn^{4+} beyond 0.5 mol.%. The decrease of PL intensity may be due to concentration quenching mechanism. This can be explained as follows: when the concentration of Mn increases, the replacement of ions Mn^{4+} on the location of the ion Al^{3+} ion host lattice crystal is also increased, leading to the emission center density increases and the result enhances fluorescence emission intensity of the sample until it reaches a maximum at 0.5 mol.%. When doping concentration increases continued to rise above 0.5 mol.%, fluorescence intensity tends to decrease. The decrease of PL intensity is due to phenomenon of energy transfer within the nearest emission centers (Mn^{4+}) that is finally transferred to nonradiative centers. Thus, the doping concentration is higher, probability of energy transfer is larger and PL intensity decreases.

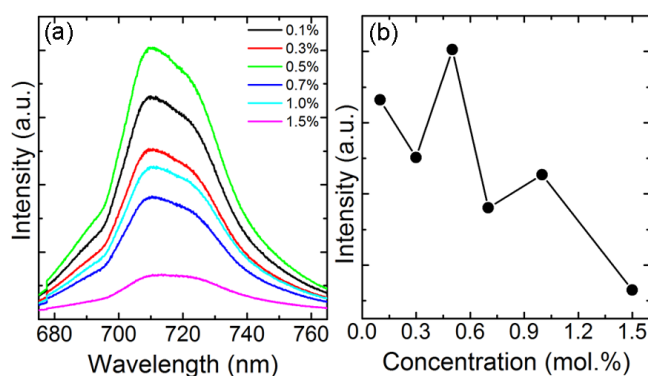


Figure 6. (a) PL spectra of $\text{CaYAIO}_4:\text{xMn}$ ($x = 0.1, 0.3, 0.5, 0.7, 1,$ and 1.5 mol.%) annealed at $1300\text{ }^\circ\text{C}$ excited at 320 nm , (b) PL intensity at 710 nm as function of Mn^{4+} concentration.

4. CONCLUSIONS

In summary, far-red emitting $\text{CaYAIO}_4:\text{Mn}^{4+}$ phosphor was successfully synthesized by co-precipitation method coupled with various annealing temperature from $800\text{ }^\circ\text{C}$ to $1300\text{ }^\circ\text{C}$ for 5 h. For phase, morphology and optical properties of the phosphor, the effects of annealing temperature were investigated in detail. XRD patterns confirm that the obtained samples are single phase (CaYAIO_4). Under the excitation at 320 nm , the $\text{CaYAIO}_4:\text{Mn}^{4+}$ phosphors exhibited far-red emission peaking at 710 nm , which is attributed to the spin-forbidden ${}^2E_g \rightarrow {}^4A_{2g}$ transition of Mn^{4+} ions. This phosphor is effectively excited by UV or blue LED chip and emits far-red light. CaYAIO_4 doped with $0.5\text{ mol.}\%$ Mn^{4+} showed the highest luminescence intensity. With the optical properties of the phosphor pointed out that the as-prepared $\text{CaYAIO}_4:\text{Mn}^{4+}$ could be applied in indoor plant growth illumination.

Acknowledgements. The present research was supported by a grant from the Vietnamese Ministry of Education and Training under grant number B2019-BKA-08.

REFERENCES

1. Huang X., Li B., Guo H., and Chen D. - Molybdenum-doping-induced photoluminescence enhancement in Eu^{3+} -activated CaWO_4 red-emitting phosphors for white light-emitting diodes, *Dyes Pigments* **143** (2017) 86–94.

2. Cao R., Chen G., Yu X., Tang P., Luo Z., Guo S., Zheng G. - Enhanced photoluminescence of $\text{CaTiO}_3:\text{Sm}^{3+}$ red phosphors by Na^+ , H_3BO_3 added, *Mater. Chem. Phys.* **171** (2016) 222-226.
3. Du P., Yu J.S. - Synthesis and luminescent properties of Eu^{3+} -activated $\text{Na}_{0.5}\text{Gd}_{0.5}\text{MoO}_4$: A strong red-emitting phosphor for LED and FED applications, *J. Lumin.* **179** (2016) 451-456.
4. Du P., Guo Y., Lee S.H., Yu J.S. - Broad near-ultraviolet and blue excitation band induced dazzling red emissions in Eu^{3+} -activated Gd_2MoO_6 phosphors for white light-emitting diodes, *RSC Adv.* **7** (2017) 3170-3178.
5. Devakumar B., Halappa P., Shivakumara C. - $\text{Dy}^{3+}/\text{Eu}^{3+}$ co-doped $\text{CsGd}(\text{MoO}_4)_2$ phosphor with tunable photoluminescence properties for near-UV WLEDs applications, *Dyes Pigments* **137** (2017) 244-255.
6. Srivastava A.M., Camardello S.J., Brik M.G. - Luminescence of Mn^{4+} in the orthorhombic perovskite, LaGaO_3 , *J. Lumin.* **183** (2017) 437-441.
7. Cao R., Wang W., Zhang J., Jiang S., Chen Z., Li W., Yu X. - Synthesis and luminescence properties of $\text{Li}_2\text{SnO}_3:\text{Mn}^{4+}$ red-emitting phosphor for solid-state lighting, *J. Alloy Compd.* **704** (2017) 124-130.
8. Blasse G., Grabmaier B.C. - *Luminescent Materials*, Springer-Verlag, Berlin-Heidelberg (1994).
9. Lu W., Lv W., Zhao Q., Jiao M., Shao B., You H. - A novel efficient Mn^{4+} activated $\text{Ca}_{14}\text{Al}_{10}\text{Zn}_6\text{O}_{35}$ phosphor: application in red-emitting and white LEDs, *Inorg. Chem.* **53** (2014) 11985-11990.
10. Sun Q., Wang S., Li B., Guo H., Huang X. - Synthesis and photoluminescence properties of deep red-emitting $\text{CaGdAlO}_4:\text{Mn}^{4+}$ phosphors for plant growth LEDs, *J. Lumin.* **203** (2018) 371-375.
11. Wang B., Lin H., Xu J., Chen H., Wang Y. - $\text{CaMg}_2\text{Al}_{16}\text{O}_{27}:\text{Mn}^{4+}$ -based Red Phosphor: A potential color converter for high-powered warm w-LED, *ACS Appl. Mater. Interfaces* **6** (2014) 22905-22913.
12. Park J.Y., Joo J.S., Yang H.K., Kwak M. - Deep red-emitting $\text{Ca}_{14}\text{Al}_{10}\text{Zn}_6\text{O}_{35}:\text{Mn}^{4+}$ phosphors for WLED applications, *J. Alloys Compd.* **714** (2017) 390-396.
13. Zhang Y., Li X., Li K., Lian H., Shang M., Lin J. - Crystal-site engineering control for the reduction of Eu^{3+} to Eu^{2+} in CaYAlO_4 : structure refinement and tunable emission properties, *ACS Appl. Mater. Interfaces* **7** (2015) 2715-2725.
14. Lv S., Zhu Z., Wang Y., You Z., Li J., Tu C. - Spectroscopic investigations of $\text{Ho}^{3+}/\text{Er}^{3+}:\text{CaYAlO}_4$ and $\text{Eu}^{3+}/\text{Er}^{3+}:\text{CaYAlO}_4$ crystals for 2.7 μm emission, *J. Lumin.* **144** (2013) 117-121.
15. Shannon R.D. - Revised effective ionic radii and systematic studies of interatomic distances in halides and chalcogenides. *Acta Crystallogr.* **A32** (1976) 751-767.
16. Sun Q., Wang S., Devakumar B., Sun Y., Liang J., Huang X., Wu Y. - $\text{CaYAlO}_4:\text{Mn}^{4+},\text{Mg}^{2+}$: An efficient far-red-emitting phosphor for indoor plant growth LEDs, *J. Alloys Compd.* **758** (2019) 1198-1205.